Single chargino production with R-parity lepton number violation in photon-photon collisions

Yin Xi[a], Ma Wen-Gan[a], Wan Lang-Hui[a], Jiang Yi[a] and Han Liang[a]

[a]Modern Physics Department, University of Science and Technology of China, Anhui 230027, China.

Abstract

We examine the process $\gamma\gamma \to \tilde{\chi}^+\tau^-$ at photon-photon collider in the minimal supersymmetric standard model(MSSM) with R-parity violation, where all the one-loop diagrams are considered. We mainly discuss the effects of bilinear breaking terms, and conclude that their contributions may be important compared with trilinear terms. Our results show that the events of this process could be detectable at photon-photon colliders, if the values of the parameters are favorable.

PACS: 11.30.Er, 12.60.Jv, 14.80.Ly
Key word: R-parity violation, single chargino production, lepton number violation, photon-photon collision

I. Introduction

The new physics beyond the standard model (SM) has been intensively studied in past years[1]. The supersymmetric models (SUSY) are the most attractive ones among general extended models of the SM. As we know that electroweak gauge invariance requires the absence of terms in the lagrangian that change either baryon number or lepton number. Usually these terms may lead to an unacceptable short proton lifetime. One way to solve the proton-decay problem is to impose a discrete symmetry conservation called R-parity (R_p) conservation[2]. Actually conservation of R-parity is put into the MSSM in order to ensure retaining symmetries of the SM. But the most general supersymmetric (SUSY) extension of the SM should contain such terms.

If R-parity is conserved, all supersymmetric partner particles must be produced in pair, thus the lightest of superparticles must be stable. If R-parity is violated, the feature of SUSY models is changed a lot. Until now we have being lacking in credible theoretical argument and experimental tests for R_p conservation, we can say that the R_p violation ($\not{R}_p$) would be equally well motivated in the supersymmetric extension of the SM. Even if we failed in finding a direct signal of the MSSM in the experiments, it would be also significant to obtain a signal on R_p violation, which has recently motivated some investigation[3] [4] [5] because of experimentally observed discrepancies.

Experimentally searching for the effects of $\not{R}_p$ interactions has been done with many efforts in the last few years. Unfortunately, up to now we have only some upper limits on $\not{R}_p$ parameters. It is necessary to continue these works on finding $\not{R}_p$ signal or putting further stringent constraints on the $\not{R}_p$ parameters in future experiments. The popular way to find a $\not{R}_p$ violating signal is to detect the decay of the lightest supersymmetric particle(LSP)[6], which is difficult experimentally especially at photon colliders. The best signature for $\not{R}_p$ at future Linear Colliders (LC) is the resonant Higgs and sneutrino production through the bilinear $\not{R}_p$ parameters ϵ and the trilinear parameters λ or λ', respectively. The linear collider operating in photon collision mode has a distinct advantage over the situation at the pure e^+e^- process, where the search of narrow resonances requires lengthy scans over a large center of mass energy range of the machine. Similar with the situations at hadron colliders, the incoming photons (incoming partons at hadron colliders) with the continuative c.m.s. energy distribution, the resonance can be probed

over a rather wide mass range[5][7]. Then a single chargino can be produced by the Higgs (sneutrino) decays, which can be measured through the detection of its three-leptons signature. In the papers of Ref.[5][7] it is shown that the single chargino production cross section can be several hundred femto barn at the LHC.

There are two kinds of $\not{R}_p$ parameters, appearing in the bilinear terms and the trilinear terms respectively. The bilinear terms account for the mass of neutrinos, and also bring complexity into the model. Their contribution to $\not{R}_p$ process were generally believed to be unimportant, thus simply neglected in most recent works[4]. Recently M. Chaichian, K. Huitu and Z.-H. Yu studied the process $\gamma\gamma \to \tilde{\nu} \to \tilde{\chi}^{\pm} l^{\mp}$ considering only the trilinear $\not{R}_p$ terms[8]. However, in this paper we shall examine the contributions of both kinds of R-parity violation parameters, and investigate whether the contribution from bilinear terms can be considerable, even larger than that from trilinear terms with suitable parameters.

In this paper, we investigate the single chargino production process via photon-photon collisions at linear colliders (LC) operating at the energy ranging from 500 GeV to 1 TeV. We discuss this process in framework of the MSSM with R-parity lepton number violation. The paper is organized as follows: The general structure of the model and definitions are presented in Sec II. In Sec III, there are details of calculation. Numerical results and discussion are given in Sec IV. In Sec V, there is a short summary. Appendix A contains some explicit expressions used in our paper, and finally relevant Feynman rules are collected in Appendix B.

II. General Structure of the Model

Supersymmetric Yang-Mills theories contain gauge multiplets (λ^a, A^a_μ) in the adjoint representation of a gauge group G and matter multiplets (A_i, ψ_i) in some chosen representations of G. The general lagrangian of MSSM can be written as

$$\begin{aligned} \mathcal{L} &= -\tfrac{1}{4} \upsilon^a_{\mu\nu} \upsilon^{a\mu\nu} - i\bar{\lambda}^a \bar{\sigma}^\mu D_\mu \lambda^a - \tfrac{1}{2} D^a D^a - F_i^* F_i - D_\mu A_i^* D^\mu A_i - i\bar{\psi}_i \bar{\sigma}^\mu D_\mu \psi_i \\ &\quad + i\sqrt{2} g (A_i^* T^a \psi_i \lambda^a - \bar{\lambda}^a T^a A_i \bar{\psi}_i) + \mathcal{L}_{Yukawa} \end{aligned} \tag{1}$$

where

$$\begin{array}{l} D_\mu A_i = \partial_\mu A_i + igA^a_\mu T^a A_i, \\ D_\mu \psi_i = \partial_\mu \psi_i + igA^a_\mu T^a \psi_i, \\ D_\mu \lambda^a = \partial_\mu \lambda^a - g f^{abc} A^b_\mu \lambda^c \\ \upsilon^a_{\mu\nu} = \partial_\mu A^a_\nu - \partial_\nu A^a_\mu - g f^{abc} A^b_\mu A^c_\nu, \\ F_i = \frac{\partial \mathcal{W}}{\partial \Phi_i}\Big|_{\theta\theta}, \\ D^a = g A_i T^a_{ij} A_j, \\ \mathcal{L}_{Yukawa} = -\frac{1}{2}\left(\frac{\partial^2 \mathcal{W}}{\partial A_i \partial A_j}\psi_i \psi_j + h.c.\right) \end{array} \tag{2}$$

T^a is the generator of gauge group G. $\mathcal{W}$ is superpotential. Its general form for the R-parity relaxed MSSM can be written as

$$\mathcal{W} = \mathcal{W}_{MSSM} + \mathcal{W}_{\not R} \tag{3}$$

where $\mathcal{W}_{MSSM}$ denotes the R-parity conserved superpotential

$$\mathcal{W}_{MSSM} = \mu\epsilon_{ij} H^1_i H^2_j + \epsilon_{ij} l_I H^1_i \tilde{L}^I_j \tilde{R}^I - u_I (H^2_1 C^{*JI} \tilde{Q}^J_2 - H^2_2 \tilde{Q}^J_1)\tilde{U}^I - d_I (H^1_1 \tilde{Q}^I_2 - H^2_2 C^{IJ} \tilde{Q}^J_1)\tilde{D}^I \tag{4}$$

and $\mathcal{W}_{\not R}$ denotes the terms of R-parity violation.

$$W_{\not R} = \epsilon_{ij}(\lambda_{IJK} \tilde{L}^I_i \tilde{L}^J_j \tilde{R}^K + \lambda'_{IJK} \tilde{L}^I_i \tilde{Q}^J_j \tilde{D}^K + \epsilon_I H^2_i \tilde{L}^I_j) + \lambda''_{IJK} \tilde{U}^I \tilde{D}^J \tilde{D}^K \tag{5}$$

The soft breaking terms can be given by

$$\begin{array}{rcl} \mathcal{L}_{soft} & = & -m^2_{H^1} H^{1*}_i H^1_i - m^2_{H^2} H^{2*}_i H^2_i - m^2_{L^I} \tilde{L}^{I*}_i \tilde{L}^I_i - m^2_{R^I} \tilde{R}^{I*} \tilde{R}^I - m^2_{Q^I} \tilde{Q}^{I*}_i \tilde{Q}^I_i \\ & & -m^2_{D^I} \tilde{D}^{I*} \tilde{D}^I - m^2_{U^I} \tilde{U}^{I*} \tilde{U}^I + (m_1 \lambda_B \lambda_B + m_2 \lambda^i_A \lambda^i_A + m_3 \lambda^a_G \lambda^a_G + h.c.) \\ & & +\{B\mu\epsilon_{ij} H^1_i H^2_j + B_I \epsilon_I \epsilon_{ij} H^2_i \tilde{L}^I_j + \epsilon_{ij} l_{sI} H^1_i \tilde{L}^I_j \tilde{R}^I \\ & & +d_{sI}(-H^1_1 \tilde{Q}^I_2 + C^{IK} H^1_2 \tilde{Q}^K_1)\tilde{D}^I + u_{sI}(-C^{KI*} H^2_1 \tilde{Q}^I_2 + H^2_2 \tilde{Q}^I_1)\tilde{U}^I \\ & & +\epsilon_{ij} \lambda^S_{IJK} \tilde{L}^I_i \tilde{L}^J_j \tilde{R}^K + \lambda^{S'}_{IJK}(\tilde{L}^I_i \tilde{Q}^J_2 \delta^{JK} - \tilde{L}^I_2 C^{JK} \tilde{Q}^J_1)\tilde{D}^K + \lambda^{S''}_{IJK} \tilde{U}^I \tilde{D}^J \tilde{D}^K \\ & & +h.c.\} \end{array} \tag{6}$$

The bilinear $\not{R}_p$ term $\epsilon_{ij}\epsilon_I H^2_i \tilde{L}^I_j$ will lead to mixture of mass eigenstates in the R_p violating model[9], which would bring complexity into calculations. The calculation of lagrangian and corresponding Feynman rules are thus extremely complicated and tedious. The general process of computation and some useful results are summarized as following.

With this new model, physical spectrum of particles are quite different from the R_p conserved theory. The explicit expression of the mass matrix and eigenstates can be found

in Ref.[9]. We write down part of the expressions which would be useful in our following discussion. The fields of two Higgs doublets H^1, H^2 and slepton can be written as

$$H^1 = \begin{pmatrix} \frac{1}{\sqrt{2}}(\chi_1^0 + i\phi_1^0 + v_1) \\ H_2^1 \end{pmatrix} \tag{7}$$

$$H^2 = \begin{pmatrix} H_1^2 \\ \frac{1}{\sqrt{2}}(\chi_2^0 + i\phi_2^0 + v_2) \end{pmatrix} \tag{8}$$

$$\tilde{L}^I = \begin{pmatrix} \frac{1}{\sqrt{2}}(\chi_{\nu_I}^0 + i\phi_{\nu_I}^0 + v_{\nu_I}) \\ \tilde{L}_2^I \end{pmatrix} \tag{9}$$

The vacuum expectation values (VEV's) are divided from the scalar fields, written explicitly as v_1, v_2 and v_{ν_I}. From the equations above, we can find the scalar potential including a linear combination as

$$V_{tadpole} = t_1^0\chi_1^0 + t_2^0\chi_2^0 + t_{\nu_I}^0\chi_{\nu_I}^0 \tag{10}$$

where

$$\begin{aligned} t_1^0 &= \tfrac{1}{8}(g^2+g'^2)v_1(v_1^2 - v_2^2 + \textstyle\sum_I v_{\nu_I}^2) + \mid \mu \mid^2 v_1 + m_{H^1}^2 v_1 - B\mu v_2 - \textstyle\sum_I \mu\epsilon_I v_I, \\ t_2^0 &= -\tfrac{1}{8}(g^2+g'^2)v_2(v_1^2 - v_2^2 + \textstyle\sum_I v_{\nu_I}^2) + \mid \mu \mid^2 v_2 + m_{H^2}^2 v_2 - B\mu v_1 + \textstyle\sum_I \epsilon_I^2 v_2 \\ &\quad + \textstyle\sum_I B_I\epsilon_I v_I, \\ t_{\nu_I}^0 &= \tfrac{1}{8}(g^2+g'^2)v_{\nu_I}(v_1^2 - v_2^2 + \textstyle\sum_I v_{\nu_I}^2) + m_{L^I}^2 v_{\nu_I} + \epsilon_I \textstyle\sum_J \epsilon_J v_{\nu_J} - \mu\epsilon_I v_1 + B_I\epsilon_I v_2. \end{aligned} \tag{11}$$

These $t_i^0 (i = 1, 2, \nu_1, \nu_2, \nu_3)$ correspond to the tree level tadpoles, and the VEV's of the neutral scalar fields satisfy the condition $t_i^0 = 0 (i = 1, 2, \nu_1, \nu_2, \nu_3)$. Thus the neutral slepton fields generally obtain none-zero VEV's $\frac{1}{\sqrt{2}}v_{\nu_I}$, as a result of bilinear terms. The trilinear parameters alone won't contribute to the VEV's, but to $\not{R}_p$ Feynman vertices only.

We use $\chi^0 = (\chi_1^0, \chi_2^0, \chi_{\nu_1}^0, \chi_{\nu_2}^0, \chi_{\nu_3}^0)$ to denote CP-even neutral scalar fields and $\phi^0 = (\phi_1^0, \phi_2^0, \phi_{\nu_1}^0, \phi_{\nu_2}^0, \phi_{\nu_3}^0)$ to represent CP-odd neutral scalar fields. $\Phi^c = (H_2^{1*}, H_1^2,$
$\tilde{L}_2^{1*}, \tilde{L}_2^{2*}, \tilde{L}_2^{3*}, \tilde{R}^1, \tilde{R}^2, \tilde{R}^3)$ denotes the charged scalar fields. The relations between the current eigenstates and the mass eigenstates are given as

$$H_i^0 = \sum_{j=1}^{5} Z_{even}^{ij}\chi_j^0 \tag{12}$$

$$H_{5+i}^0 = \sum_{j=1}^{5} Z_{odd}^{ij}\phi_j^0 \tag{13}$$

$$H_i^+ = \sum_{j=1}^{8} Z_c^{ij} \Phi_j^c \tag{14}$$

and

$$\left(-i\lambda_B, -i\lambda_A^3, \psi_{H_1^1}, \psi_{H_2^2}, \nu_{eL}, \nu_{\mu L}, \nu_{\tau L}\right)^T = Z_N \tilde{\chi}^0 \tag{15}$$

$$\left(-i\lambda_A^+, \psi_{H_1^2}, e_R, \mu_R, \tau_R\right)^T = Z_+ \tilde{\chi}^+ \tag{16}$$

$$\left(-i\lambda_A^-, \psi_{H_2^1}, e_L, \mu_L, \tau_L\right)^T = Z_- \tilde{\chi}^- \tag{17}$$

We may formulate all the neutral fermions into four-component spinors as

$$\kappa_i^0 = \begin{pmatrix} \tilde{\chi}_i^0 \\ \bar{\tilde{\chi}}_i^0 \end{pmatrix} \tag{18}$$

and the charged fermions as

$$\kappa_i^+ = \begin{pmatrix} \tilde{\chi}_i^+ \\ \bar{\tilde{\chi}}_i^- \end{pmatrix}, \kappa_i^- = \left(\kappa_i^+\right)^c = \begin{pmatrix} \tilde{\chi}_i^- \\ \bar{\tilde{\chi}}_i^+ \end{pmatrix} \tag{19}$$

For convenience we will call all of these scalar bosons (H^1, H^2 and $\tilde{L}^I$) as Higgs (H^0 for CP-even Higgs, A^0 for CP-odd Higgs, and $H^\pm$ for charged Higgs), all charged fermions (chargino and lepton) as chargino ($\tilde{\chi}^+$), and all neutral fermions (neutralino and neutrino) as neutralino ($\tilde{\chi}^0$).

We adopt the 't Hooft-Feynman gauge, in which the Goldstone fields appear explicitly in the calculations, but ghost vertices are relatively simple. The lagrangian in terms of physical eigenstates is very complicated and tedious. For the convenience of calculation we collect the relevant Feynman rules in Appendix B.

III. Calculations

In this paper we denote the process

$$\gamma(k_1)\gamma(k_2) \longrightarrow \tilde{\chi}^+(p_1)\tau^-(p_2) \tag{20}$$

According to the MSSM of R-parity violation discussed above, there is no Feynman vertices of photon-chargino-lepton, and thus the lowest order diagrams are of one-loop. In

this case it's not necessary to consider the renormalization at one-loop level and the ultraviolet divergence should be canceled automatically if all the one-loop diagrams at the $O(m_{\tilde{\chi}_1^+} m_\tau / m_W^2)$ order in the model are included. The one-loop diagrams at the lowest order are plotted in Fig.1, where the conventions claimed in Sec II is used, such as κ_i^+ represent both chargino and lepton and so on. The diagrams exchanging the two external photon-photon lines are not shown. Fig.1(a) contains the self-energy diagrams, Fig.1(b) the vertex correction diagrams, Fig.1(c) the s-channel diagrams, Fig.1(d) the box-diagrams, and Fig.1(e) the quartic interaction diagrams.

In the calculation for the s-channel diagrams (Fig.1 c), we take into account the width effects of the H^0, A^0 and sneutrino propagators. The full calculation of mass width is complicated in the R_p-violating MSSM model. However, rough results can be obtained by some analysis. Since we set the mass of sneutrino around 400 GeV, the $t\bar{t}$ decay needs to be considered. On the other hand, for H^0 and A^0, $m_{H^0}, m_{A^0} < 2m_t$, the decay channel to $t\bar{t}$ is forbidden. Thus we consider the decay widths for sneutrinos are larger than those of Higgs, due to the large mass of m_t. For an approximate calculation, we choose $\frac{\Gamma(sneutrino)}{M(sneutrino)} = 0.15$, while $\frac{\Gamma(H^0)}{m_{H^0}} = \frac{\Gamma(A^0)}{m_{A^0}} = 0.10$ properly.

We denote θ as the scattering angle between one of the photons and the final chargino. Then we express all the four-momenta of the initial and final particles in the center-of-mass (CMS) by means of the total energy $\sqrt{\hat{s}}$ and the scattering angle θ. The four-momenta of chargino and tau are p_1 and p_2 respectively and are read

$$p_1 = \left(E_{\tilde{\chi}}, \sqrt{E_{\tilde{\chi}}^2 - m_{\tilde{\chi}}^2}\sin\theta, 0, \sqrt{E_{\tilde{\chi}}^2 - m_{\tilde{\chi}}^2}\cos\theta\right) \tag{21}$$

$$p_2 = \left(E_\tau, -\sqrt{E_\tau^2 - m_\tau^2}\sin\theta, 0, \sqrt{E_\tau^2 - m_\tau^2}\cos\theta\right) \tag{22}$$

where

$$E_{\tilde{\chi}} = \frac{1}{2}(\sqrt{\hat{s}} + (m_{\tilde{\chi}}^2 - m_\tau^2)/\sqrt{\hat{s}}) \tag{23}$$

$$E_\tau = \frac{1}{2}(\sqrt{\hat{s}} - (m_{\tilde{\chi}}^2 - m_\tau^2)/\sqrt{\hat{s}}) \tag{24}$$

p_3 and p_4 are the four-momenta of the initial photons and are expressed as

$$p_3 = (\frac{1}{2}\sqrt{\hat{s}}, 0, 0, \frac{1}{2}\sqrt{\hat{s}}) \tag{25}$$

$$p_4 = (\frac{1}{2}\sqrt{\hat{s}}, 0, 0, -\frac{1}{2}\sqrt{\hat{s}}) \tag{26}$$

The corresponding matrix element for all the diagrams in Fig.1 is written in the form

$$
\begin{aligned}
M &= M^s + M^{tr} + M^b + M^q = M^{s,\hat{t}} + M^{s,\hat{u}} + M^{tr,\hat{t}} + M^{tr,\hat{u}} + M^q \\
&= \epsilon^{\mu}(p_1)\epsilon^{\nu}(p_2)\bar{u}(k_1)\{f_1 g_{\mu\nu} + f_2\gamma_5 g_{\mu\nu} + f_3\gamma_\mu k_{1,\nu} + f_4 g_{\mu\nu}\not{p}_2 + f_5 k_{1,\nu}\gamma_5\gamma_\mu + \\
&\quad f_6 g_{\mu\nu}\gamma_5\not{p}_2 + f_7\gamma_\mu\gamma_\nu + f_8\gamma_5\gamma_\mu\gamma_\nu + f_9\gamma_\mu\gamma_\nu\not{p}_2 + f_{10}\gamma_5\gamma_\mu\gamma_\nu\not{p}_2 + f_{11}k_{1,\mu}k_{1,\nu} + \\
&\quad f_{12}\gamma_5 k_{1,\mu}k_{1,\nu} + f_{13}\gamma_\nu k_{1,\mu} + f_{14}g_{\mu\nu}\not{p}_1 + f_{15}k_{1,\mu}\gamma_5\gamma_\nu + f_{16}g_{\mu\nu}\gamma_5\not{p}_1 + f_{17}k_{1,\nu}\gamma_\mu\not{p}_1 + \\
&\quad f_{18}k_{1,\mu}\gamma_\nu\not{p}_2 + f_{19}g_{\mu\nu}\not{p}_1\not{p}_2 + f_{20}k_{1,\nu}\gamma_5\gamma_\mu\not{p}_1 + f_{21}k_{1,\mu}\gamma_5\gamma_\nu\not{p}_2 + f_{22}g_{\mu\nu}\gamma_5\not{p}_1\not{p}_2 + \\
&\quad f_{23}\gamma_\mu\gamma_\nu\not{p}_1 + f_{24}\gamma_5\gamma_\mu\gamma_\nu\not{p}_1 + f_{25}\gamma_\mu\gamma_\nu\not{p}_1\not{p}_2 + f_{26}\gamma_5\gamma_\mu\gamma_\nu\not{p}_1\not{p}_2 + f_{27}k_{1,\mu}k_{1,\nu}\not{p}_1 + \\
&\quad f_{28}k_{1,\mu}k_{1,\nu}\gamma_5\not{p}_1 + f_{29}k_{1,\mu}\gamma_\nu\not{p}_1 + f_{30}k_{1,\mu}\gamma_5\gamma_\nu\not{p}_1 + f_{31}k_{1,\mu}\gamma_\nu\not{p}_1\not{p}_2 + f_{32}k_{1,\mu}\gamma_5\gamma_\nu\not{p}_1\not{p}_2 + \\
&\quad f_{33}\gamma_\mu p_{1,\nu} + f_{34}\gamma_5\gamma_\mu p_{1,\nu} + f_{35}k_{1,\mu}p_{1,\nu} + f_{36}\gamma_5 k_{1,\mu}p_{1,\nu} + f_{37}\gamma_\mu\not{p}_1 p_{1,\nu} + \\
&\quad f_{38}\gamma_\mu\not{p}_2 p_{1,\nu} + f_{39}\gamma_5\gamma_\mu\not{p}_1 p_{1,\nu} + f_{40}\gamma_5\gamma_\mu\not{p}_2 p_{1,\nu} + f_{41}k_{1,\mu}k_{1,\nu}\not{p}_2 + f_{42}k_{1,\mu}k_{1,\nu}\gamma_5\not{p}_2 + \\
&\quad f_{43}k_{1,\nu}\gamma_\mu\not{p}_2 + f_{44}k_{1,\nu}\gamma_5\gamma_\mu\not{p}_2 + f_{45}k_{1,\nu}\gamma_\mu\not{p}_1\not{p}_2 + f_{46}k_{1,\nu}\gamma_5\gamma_\mu\not{p}_1\not{p}_2 + f_{47}k_{1,\mu}p_{1,\nu}\not{p}_2 + \\
&\quad f_{48}k_{1,\mu}\gamma_5\not{p}_2 p_{1,\nu} + f_{49}\gamma_\mu\not{p}_1\not{p}_2 p_{1,\nu} + f_{50}\gamma_5\gamma_\mu\not{p}_1\not{p}_2 p_{1,\nu} + f_{51}g_{\mu\nu}\gamma_5\not{p}_1 + f_{52}k_{1,\mu}p_{1,\nu}\not{p}_1 + \\
&\quad f_{53}k_{1,\mu}\gamma_5\not{p}_1 p_{1,\nu} + f_{54}g_{\mu\nu}\not{p}_1\not{p}_2 + f_{55}g_{\mu\nu}\gamma_5\not{p}_1\not{p}_2 + f_{56}\epsilon_{\alpha\beta\mu\nu}p_1^\alpha p_2^\beta + f_{57}\gamma_5\epsilon_{\alpha\beta\mu\nu}p_1^\alpha p_2^\beta + \\
&\quad f_{58}\epsilon_{\alpha\beta\mu\nu}\gamma^\alpha p_1^\beta + f_{59}\epsilon_{\alpha\beta\mu\nu}\gamma^\alpha p_2^\beta + f_{60}\epsilon_{\alpha\beta\mu\nu}p_1^\alpha p_2^\beta\not{p}_1 + f_{61}\epsilon_{\alpha\beta\mu\nu}p_1^\alpha p_2^\beta\not{p}_2 + \\
&\quad f_{62}\gamma_5\epsilon_{\alpha\beta\mu\nu}\gamma^\alpha p_1^\beta + f_{63}\gamma_5\epsilon_{\alpha\beta\mu\nu}\gamma^\alpha p_2^\beta + f_{64}\epsilon_{\alpha\beta\mu\nu}p_1^\alpha p_2^\beta\gamma_5\not{p}_1 + f_{65}\epsilon_{\alpha\beta\mu\nu}p_1^\alpha p_2^\beta\gamma_5\not{p}_2 + \\
&\quad f_{66}\epsilon_{\alpha\beta\gamma\mu}\gamma^\alpha p_1^\beta p_2^\gamma p_{1,\nu} + f_{67}\gamma_5\epsilon_{\alpha\beta\gamma\mu}\gamma^\alpha p_1^\beta p_2^\gamma p_{1,\nu} + f_{68}\gamma_\nu k_{2,\mu} + f_{69}k_{2,\mu}\gamma_5\gamma_\nu + f_{70}\gamma_\mu k_{2,\nu} + \\
&\quad f_{71}k_{2,\nu}\gamma_5\gamma_\mu\}v(k_2)
\end{aligned}
\tag{27}
$$

The variables $\hat{s}$, $\hat{t}$ and $\hat{u}$ are usual Mandelstam variables in the center of mass system of photon-photon, defined as

$$\hat{s} = (p_1 + p_2)^2 = (p_3 + p_4)^2 \tag{28}$$

$$\hat{t} = (p_1 - p_3)^2 = (p_2 - p_4)^2 \tag{29}$$

$$\hat{u} = (p_1 - p_4)^2 = (p_2 - p_3)^2 \tag{30}$$

Explicit expressions of the factors f_i appearing in Eq.(27) are very complicated and tedious, thus we do not list them in our paper. The total cross section for the subprocess $\gamma\gamma \to \tilde{\chi}^+\tau^-$ can be written in the form as

$$\hat{\sigma}(\hat{s}) = \frac{1}{16\pi\hat{s}^2}\int_{\hat{t}^-}^{\hat{t}^+} d\hat{t} \mid \bar{M} \mid^2 \tag{31}$$

where $\mid \bar{M} \mid^2$ is the initial spin-averaged matrix element squared and $\hat{t}^{\pm} = \frac{1}{2}(m_{\tilde{\chi}}^2 + m_\tau^2 - \hat{s}) \pm \sqrt{E_{\tilde{\chi}}^2 - m_{\tilde{\chi}}^2}\sqrt{\hat{s}}$.

With the integrated photon luminosity in the e^+e^- collisions, the total cross section of the process $e^+e^- \to \gamma\gamma \to \tilde{\chi}^+\tau^-$ can be written as

$$\sigma(s) = \int_{(m_{\tilde{\chi}}+m\tau)/\sqrt{\hat{s}}}^{x_{max}} dz \frac{d\mathcal{L}_{\gamma\gamma}}{dz}\hat{\sigma}(\gamma\gamma \to \tilde{\chi}^+\tau^- at \hat{s} = z^2 s) \tag{32}$$

where $\sqrt{s}$ and $\sqrt{\hat{s}}$ are the total energy of the center-of-mass of e^+e^- and $\gamma\gamma$ respectively. $\frac{d\mathcal{L}_{\gamma\gamma}}{dz}$ is defined as

$$\frac{d\mathcal{L}_{\gamma\gamma}}{dz} = 2z \int_{z^2/x_{max}}^{x_{max}} \frac{dx}{x} F_{\gamma/e}(x) F_{\gamma/e}(z^2/x) \tag{33}$$

For the initial unpolarized electrons and laser photon beams, the energy spectrum of the back-scattered is given by[11]

$$F_{\gamma/e} = \frac{1}{D(\xi)} \left[1 - x + \frac{1}{1-x} - \frac{4x}{\xi(1-x)} + \frac{4x^2}{\xi^2(1-x)^2} \right] \tag{34}$$

where

$$D(\xi) = (1 - \frac{4}{\xi} - \frac{8}{\xi^2}) \ln(1+\xi) + \frac{1}{2} + \frac{8}{\xi} - \frac{1}{2(1+\xi)^2} \tag{35}$$

$$\xi = 4E_0\omega_0/m_e^2 \tag{36}$$

where m_e and E_0 are the mass and energy of the electron respectively, x represents the fraction of the energy of the incident electron carried by the back-scattered photon. In our evaluation, we choose ω_0 such that it maximizes the backscattered photon energy without spoiling the luminosity by e^+e^- pair production. Then we get $\xi = 2(1+\sqrt{2}) \simeq 4.8, x_{max} \simeq 0.83$ and $D(\xi) \simeq 1.8$, a usual method used in Ref.[12].

IV. Numerical Calculations and Discussions

In the numerical computation we use input parameters as $m_b = 4.5GeV, m_c = 1.35GeV, m_t = 175GeV, M_W = 80.2226GeV, G_F = 1.166392 \times 10^{-5}(GeV)^{-2}$ and $\alpha = 1/137.036$[13].

Although there are some constraints on the supersymmetric parameters in some theory, such as the minimal supergravity (mSUGRA), in the following analysis we do not put any extra limitations on them for the general discussion. In the numerical calculation, we set the following parameters arbitrarily, in case that no special declaration has been presented on them.

$$\begin{aligned} &\tan\beta = 5, \quad m_{L^I} = 400\ GeV \\ &m_{Q^{1,2}} = m_{D^{1,2}} = m_{U^{1,2}} = 600\ GeV \\ &m_{Q^3} = 400\ GeV, \quad m_{D^3} = 500\ GeV, \quad m_{U^3} = 300\ GeV \end{aligned} \tag{37}$$

where $m_{L^I}, m_{Q^I}, m_{D^I}, m_{U^I}$ are the soft-breaking masses appeared in Eq.(6). We choose m_2 in the range from 45 GeV to 150 GeV, and μ from 100 GeV to 370 GeV. If we omit R_p breaking, the chargino mass matrix can be written as

$$M_{\tilde{\chi}^+} = \begin{pmatrix} 2m_2 & \frac{1}{\sqrt{2}}gv_1 \\ \frac{1}{\sqrt{2}}gv_2 & -\mu \end{pmatrix} \tag{38}$$

In the case of large μ, mass of $\tilde{\chi}_1^+$ is close to $2m_2$. The $\not{R}_p$ parameters are taken as follows

$$\begin{array}{l} \epsilon_1 = \epsilon_2 = 0, \quad \epsilon_3 = 10\ GeV \\ v_{\nu_1} = v_{\nu_2} = 0, \quad v_{\nu_3} = -4.7\ GeV \end{array} \tag{39}$$

and

$$\begin{array}{l} \lambda_{131} = 0.05, \quad \lambda_{232} = 0.09 \\ \lambda'_{ijk} = 0.1, \quad \lambda''_{ijk} = 0 \end{array} \tag{40}$$

The first two indices for parameters λ_{ijk} are antisymmetric, or written explicitly, $\lambda_{ijk} = -\lambda_{jik}$. For the rest of parameters which are not given in Eq.(38), we set $\lambda_{ijk} = 0$ assuming the $\not{R}_p$ for the first two generations can be neglected. Since we mainly investigate the effects of bilinear breaking parameters ϵ, trilinear parameters are generally assumed to be vanished without emphasis.

In Fig.2 we depict the dependences of $\gamma\gamma \to \tilde{\chi}^+\tau^-$ subprocess cross section on the c.m. energy $\sqrt{\hat{s}}$, where the contributions from all diagrams with effects of only bilinear terms are included. The masses of the final chargino are set as 90 GeV, 110 GeV and 170 GeV respectively. Generally two peaks at $\sqrt{\hat{s}} \sim m_{H^0} \simeq 290\ GeV$ and $\sqrt{\hat{s}} \sim m_{\tilde{\nu}} \simeq 390\ GeV$ can be seen, as the result of resonance effects through decays of H^0, A^0 and $\tilde{\nu}$. When the mass of $\tilde{\chi}_1$ decreases to 90 GeV, which is close to the mass of h^0, the cross section is enhanced considerably by resonance effect. The small peak of the solid line, where $\sqrt{\hat{s}} \sim 2m_W, 2m_{h^0} \simeq 174\ GeV$, comes from the contribution of the resonant effects of box and quartic vertex diagrams including W^+ and h^0 particles. For comparison we also calculated the contributions of the diagrams with the couplings induced from only the trilinear breaking terms. In this case neutral Higgs decay to $\tilde{\chi}_1^+\tau^-$ is forbidden, thus we take into account only $\tilde{\nu}$ decay channel. Their contributions can be typically 1-2 orders lower than those of bilinear terms, which is not plotted explicitly.

The cross sections of the $e^+e^- \to \gamma\gamma \to \tilde{\chi}_1^+\tau^-$ process and the $e^+e^- \to \tilde{\chi}_1^+\tau^-$ tree level process are plotted as functions of $\sqrt{s}$ in Fig.3 neglecting the contributions from the trilinear terms. Fig.3 shows that when $m_{\tilde{\chi}_1} = 90GeV$, the $\gamma\gamma$ one-loop cross section has its maximum at 0.39 fb. The cross section of the e^+e^- tree level process has been

calculated in Ref.[9]. According to our results in Fig.3, $\sigma_{Born}(e^+e^- \to \tilde{\chi}_1^+\tau^-)$ ranges from 0.1 fb to 0.5 fb when mass of $\tilde{\chi}_1^+$ varies from 190 GeV to 90 GeV. We have $\sigma(e^+e^- \to \gamma\gamma \to \tilde{\chi}_1^+\tau^-)/\sigma(e^+e^- \to \tilde{\chi}_1^+\tau^-) \simeq 10^{-1} - 1$. It shows that contributions of the one-loop level $\gamma\gamma$ process can be comparable with the tree level e^+e^- process, thus a possible way to detect single chargino production.

In Fig.4 we depict the cross section of the e^+e^- process versus the final chargino mass $m_{\tilde{\chi}_1}$, where $\mu = 370\ GeV$. We choose the c.m. collision energy $\sqrt{s}$ at 500 GeV and 1000 GeV, and $m_{\tilde{\chi}_1}$ ranges from 90 GeV to 200 GeV. The cross section decreases as $m_{\tilde{\chi}_1}$ rises, ranging from 0.39 fb to 0.01 fb.

The dependence of the cross sections on parameter μ is plotted in Fig.5, where $m_2 = 150\ GeV$. We choose $\sqrt{s}$ at 500 GeV and 1000 GeV respectively. The variety of μ has effects on m_{H^0} and $m_{\tilde{\chi}_1}$, thus on the contribution of resonance effects. While μ ranges from 100 GeV to 300 GeV, the cross section starts at 0.61 fb ($\sqrt{s} = 500\ GeV$), drops rapidly till $\mu = 150\ GeV$, then decreases slower, ended at 0.008 fb.

V.Summary

In this work we have studied the $\not{R}_p$ process $e^+e^- \to \gamma\gamma \to \tilde{\chi}_1^+\tau^-$ in the framework of R-parity relaxed MSSM, concerning mainly bilinear parameters. We investigated the dependence of the cross section on c.m. energy $\sqrt{s}$, mass of $\tilde{\chi}_1^+$ and μ. Contributions of bilinear breaking terms and trilinear terms with typical parameters are compared. Our results show that it is contrary to the general expectation, bilinear terms account for most of the contribution in our calculation, which bring more diagrams into consideration, including neutral Higgs s-channel diagrams. For LC operating at c.m.s. energy of 500 GeV with 50 fb^{-1} integrated luminosity, one can expect a typical rate of 11 raw events when $M_{\tilde{\chi}_1} = 100GeV$. That means the $\tilde{\chi}_1^+\tau^-$ production may be detectable at future LC.

Acknowledgement: This work was supported in part by the National Natural Science Foundation of China(project numbers: 19675033,10005009), the Education Ministry of China and the State Commission of Science and Technology of China.

Appendix A: Definitions in the Calculation

$$
\begin{aligned}
A^{i}_{ve} &= v_1 Z^{i,1}_{even} - v_2 Z^{i,2}_{even} + v_{\nu_I} Z^{i,2+I}_{even} \\
A^{ij}_{ec} &= Z^{i,1}_{even} Z^{j,1}_{c} + Z^{i,2}_{even} Z^{j,2}_{c} + Z^{i,2+I}_{even} Z^{j,2+I}_{c} \\
A^{ij}_{oc} &= Z^{i,1}_{odd} Z^{j,1}_{c} - Z^{i,2}_{odd} Z^{j,2}_{c} + Z^{i,2+I}_{odd} Z^{j,2+I}_{c} \\
A^{ij}_{cc} &= Z^{i,1}_{c} Z^{j,1}_{c} - Z^{i,2}_{c} Z^{j,2}_{c} + Z^{i,2+I}_{c} Z^{j,2+I}_{c} \\
A^{ijk}_{ecc} &= \frac{1}{4}\{-(g^2 - g'^2) A^{jk}_{cc} A^{i}_{ve} + g^2 [v_1 (A^{ik}_{ec} Z^{j,1}_{c} + A^{ij}_{ec} Z^{k,1}_{c}) + v_2 (A^{ik}_{ec} Z^{j,2}_{c} + A^{ij}_{ec} Z^{k,2}_{c}) \\
&\quad + v_{\nu_I} (A^{ik}_{ec} Z^{j,2+I}_{c} + A^{ij}_{ec} Z^{k,2+I}_{c})] - 2 g'^2 A^{i}_{ve} Z^{j,5+I}_{c} Z^{k,5+I}_{c} \\
&\quad - 2 l_I^2 [(Z^{j,2+I}_{c} Z^{k,1}_{c} + Z^{j,1}_{c} Z^{k,2+I}_{c})(v_{\nu_I} Z^{i,1}_{even} + v_1 Z^{i,2+I}_{even}) \\
&\quad - 2 v_1 (Z^{j,2+I}_{c} Z^{k,2+I}_{c} + Z^{j,5+I}_{c} Z^{k,5+I}_{c}) Z^{i,1}_{even} - 2 v_{\nu_I} Z^{j,1}_{c} Z^{k,1}_{c} Z^{i,2+I}_{even}] \\
&\quad - 2\sqrt{2} \mu l_{sI} [(Z^{k,5+I}_{c} Z^{j,2+I}_{c} + Z^{k,2+I}_{c} Z^{j,5+I}_{c}) Z^{i,1}_{even} - (Z^{j,5+I}_{c} Z^{j,1}_{c} + Z^{k,1}_{c} Z^{j,5+I}_{c}) Z^{i,2+I}_{even}] \\
&\quad + 2\sqrt{2} \mu l_I [(Z^{k,5+I}_{c} Z^{j,2+I}_{c} + Z^{k,2+I}_{c} Z^{j,5+I}_{c}) Z^{i,2}_{even} + (Z^{k,5+I}_{c} Z^{j,2}_{c} + Z^{k,2}_{c} Z^{j,5+I}_{c}) Z^{i,2+I}_{even}] \\
&\quad + 2\sqrt{2} l_I \epsilon_I [(Z^{k,5+I}_{c} Z^{j,1}_{c} + Z^{k,1}_{c} Z^{j,5+I}_{c}) Z^{i,2}_{even} + (Z^{k,5+I}_{c} Z^{j,2}_{c} + Z^{k,2}_{c} Z^{j,5+I}_{c}) Z^{i,1}_{even}] \\
&\quad + 2 l_I l_J Z^{j,5+J}_{c} Z^{k,5+I}_{c} (v_{\nu_J} Z^{i,2+I}_{even} + v_{\nu_I} Z^{i,2+J}_{even})\} \\
A^{ijk}_{occ} &= \frac{1}{4}\{g^2 [v_1 (A^{ik}_{oc} Z^{j,1}_{c} - A^{ij}_{oc} Z^{k,1}_{c}) + v_2 (A^{ik}_{oc} Z^{j,2}_{c} - A^{ij}_{oc} Z^{k,2}_{c}) \\
&\quad + v_{\nu_I} (A^{ik}_{oc} Z^{j,2+I}_{c} - A^{ij}_{oc} Z^{k,2+I}_{c})] \\
&\quad + 2 l_I^2 (Z^{j,2+I}_{c} Z^{k,1}_{c} - Z^{j,1}_{c} Z^{k,2+I}_{c})(-v_{\nu_I} Z^{i,1}_{odd} + v_1 Z^{i,2+I}_{odd}) \\
&\quad - 2\sqrt{2} \mu l_{sI} [(Z^{k,5+I}_{c} Z^{j,2+I}_{c} - Z^{k,2+I}_{c} Z^{j,5+I}_{c}) Z^{i,1}_{odd} - (Z^{k,5+I}_{c} Z^{j,1}_{c} - Z^{k,1}_{c} Z^{j,5+I}_{c}) Z^{i,2+I}_{odd}] \\
&\quad - 2\sqrt{2} \mu l_I [(Z^{k,5+I}_{c} Z^{j,2+I}_{c} - Z^{k,2+I}_{c} Z^{j,5+I}_{c}) Z^{i,2}_{odd} - (Z^{k,5+I}_{c} Z^{j,2}_{c} - Z^{k,2}_{c} Z^{j,5+I}_{c}) Z^{i,2+I}_{odd}] \\
&\quad - 2\sqrt{2} l_I \epsilon_I [(Z^{k,5+I}_{c} Z^{j,1}_{c} - Z^{k,1}_{c} Z^{j,5+I}_{c}) Z^{i,2}_{odd} - (Z^{k,5+I}_{c} Z^{j,2}_{c} - Z^{k,2}_{c} Z^{j,5+I}_{c}) Z^{i,1}_{odd}] \\
&\quad + 2 l_I l_J Z^{j,5+J}_{c} Z^{k,5+I}_{c} (v_{\nu_J} Z^{i,2+I}_{odd} - v_{\nu_I} Z^{i,2+J}_{odd})\}
\end{aligned}
$$

Appendix B: Relevant Feynman Vertices

We write down all the relevant $\not{R}_p$ Feynman vertices as follows

$$
\begin{aligned}
H^0_i - W^-_\mu - W^+_\nu &: -\frac{i}{2} g^2 A^{i}_{ve} g_{\mu\nu} \\
H^+_1 - W^-_\mu - A_\nu &: \frac{i}{2} \sqrt{g^2 + g'^2}\, m_W \sin 2\theta_W g_{\mu\nu}
\end{aligned}
$$

$$
\begin{aligned}
H_1^+ - W_\mu^+ - Z_\nu^0 &: \frac{i}{2}\sqrt{g^2+g'^2}m_W(\cos 2\theta_W - 1)g_{\mu\nu} \\
H_i^0(p_1) - \bar{H}_j^+(p_2) - W_\mu^+ &: -\frac{i}{2}gA_{ec}^{ij}(p_1+p_2)^\mu \\
H_{5+i}^0(p_1) - \bar{H}_j^+(p_2) - W_\mu^+ &: -\frac{1}{2}gA_{oc}^{ij}(p_1+p_2)^\mu \\
\bar{H}_i^+(p_1) - H_j^+(p_2) - A_\mu &: \frac{i}{2}\sqrt{g^2+g'^2}\sin 2\theta_W\delta_{ij}(p_1+p_2)^\mu \\
\bar{H}_i^+(p_1) - H_j^+(p_2) - Z_\mu^0 &: \frac{i}{2}\sqrt{g^2+g'^2}(\cos 2\theta_W\delta_{ij} - Z_c^{i,5+I}Z_c^{j,5+I})(p_1+p_2)^\mu \\
H_i^0 - \bar{H}_j^+ - A_\mu - W_\nu^+ &: \frac{i}{2}g^2\sin\theta_W A_{ec}^{ij}g_{\mu\nu} \\
H_{5+i}^0 - \bar{H}_j^+ - A_\mu - W_\nu^+ &: \frac{1}{2}g^2\sin\theta_W A_{oc}^{ij}g_{\mu\nu} \\
\bar{H}_i^+ - H_j^+ - A_\mu - A_\nu &: -\frac{i}{2}(g^2+g'^2)\sin^2 2\theta_W\delta_{ij}g_{\mu\nu} \\
\bar{H}_i^+ - H_j^+ - A_\mu - Z_\nu^0 &: -\frac{i}{2}(g^2+g'^2)[\cos 2\theta_W \sin 2\theta_W\delta_{ij} \\
&\quad -Z_c^{i,5+I}Z_c^{j,5+I}(\cos 2\theta_W \sin 2\theta_W + 4\sin^3\theta_W\cos\theta_W)]g_{\mu\nu} \\
W_\mu^+ - \kappa_j^0 - \bar{\kappa}_i^+ &: ig\gamma^\mu[(Z_+^{*i,1}Z_N^{j,2} - \frac{1}{\sqrt{2}}Z_+^{*i,2}Z_N^{j,4})P_L \\
&\quad +(Z_-^{i,1}Z_N^{*j,2} + \frac{1}{\sqrt{2}}(Z_-^{i,2}Z_N^{*j,3} + Z_-^{i,2+I}Z_N^{*j,4+I}))P_R] \\
Z_\mu^0 - \kappa_j^+ - \bar{\kappa}_i^+ &: i\sqrt{g^2+g'^2}\gamma^\mu[(-\cos^2\theta_W\delta_{ij} + \frac{1}{2}Z_+^{*i,2}Z_+^{j,2} + Z_+^{*i,2+I}Z_+^{j,2+I})P_L \\
&\quad +(-\cos^2\theta_W\delta_{ij} + \frac{1}{2}(Z_-^{i,2}Z_-^{*j,2} + Z_-^{i,2+I}Z_-^{*j,2+I}))P_R] \\
A_\mu - \kappa_j^+ - \bar{\kappa}_i^+ &: -ig\sin\theta_W\gamma^\mu\delta_{ij} \\
H_i^0 - \bar{H}_j^+ - H_k^+ &: -iA_{ecc}^{ijk} \\
H_{5+i}^0 - \bar{H}_j^+ - H_k^+ &: A_{occ}^{ijk} \\
H_i^0 - D_+^{I,j} - \bar{D}_+^{I,k} &: i\{Z_{D_I}^{*k,1}Z_{D_I}^{j,1}[\frac{1}{12}(3g^2+g'^2)A_{ve}^i - v_1 d^{I2}Z_{even}^{i,1}] \\
&\quad +Z_{D_I}^{*k,2}Z_{D_I}^{j,2}(\frac{1}{6}g'^2A_{ve}^i - v_1 d^{I2}Z_{even}^{i,1}) \\
&\quad +\frac{1}{\sqrt{2}}\mu(d^I Z_{even}^{i,2} - d_s^I Z_{even}^{i,1})(Z_{D_I}^{*k,1}Z_{D_I}^{j,2} + Z_{D_I}^{*k,2}Z_{D_I}^{j,1})\} \\
H_{5+i}^0 - D_+^{I,j} - \bar{D}_+^{I,k} &: \frac{1}{\sqrt{2}}\mu(d^I Z_{odd}^{i,2} + d_s^I Z_{odd}^{i,1})(Z_{D_I}^{*k,1}Z_{D_I}^{j,2} - Z_{D_I}^{*k,2}Z_{D_I}^{j,1})
\end{aligned}
$$

$$
\begin{aligned}
H_i^0 - U_-^{I,j} - \bar{U}_-^{I,k} \;:\; & -i\{Z_{U_I}^{*k,1} Z_{U_I}^{j,1} [\frac{1}{12}(3g^2 - g'^2) A_{ve}^i + v_2 u^{I2} Z_{even}^{i,2}] \\
& + Z_{U_I}^{*k,2} Z_{U_I}^{j,2} (\frac{1}{3} g'^2 A_{ve}^i + v_2 u^{I2} Z_{even}^{i,2}) \\
& + \frac{1}{\sqrt{2}} [\mu (u^I Z_{even}^{i,1} - u_s^I Z_{even}^{i,2}) - \epsilon_J u^I Z_{even}^{i,2+J}] \cdot \\
& (Z_{U_I}^{*k,1} Z_{U_I}^{j,2} + Z_{U_I}^{*k,2} Z_{U_I}^{j,1})\} \\
H_{5+i}^0 - U_-^{I,j} - \bar{U}_-^{I,k} \;:\; & \frac{1}{\sqrt{2}} [\mu (u^I Z_{odd}^{i,1} + u_s^I Z_{odd}^{i,2}) - \epsilon_J u^I Z_{odd}^{i,2+J}] (Z_{U_I}^{*k,2} Z_{U_I}^{j,1} - Z_{U_I}^{*k,1} Z_{U_I}^{j,2}) \\
U_-^{I,j} - \kappa_i^+ - \bar{d}^J \;:\; & -iC^{*JI} (g Z_+^{i,1} Z_{U_I}^{j,1} - u^I Z_+^{i,2} Z_{U_I}^{j,2}) P_L - iC^{*JI} d^J Z_-^{*i,2} Z_{U_I}^{j,1} P_R \\
D_+^{I,j} - \kappa_i^+ - \bar{u}^J \;:\; & -iC^{IJ} (g Z_-^{i,1} Z_{D_I}^{j,1} + d^I Z_-^{i,2} Z_{D_I}^{j,2}) P_L + iC^{IJ} u^J Z_+^{*i,2} Z_{D_I}^{j,1} P_R \\
H_j^0 - \kappa_i^+ - \bar{\kappa}_k^+ \;:\; & -\frac{i}{\sqrt{2}} [g Z_-^{k,2} Z_+^{i,1} Z_{even}^{j,1} + g Z_-^{k,1} Z_+^{i,2} Z_{even}^{j,2} + l_I Z_-^{k,2+I} Z_+^{i,2+I} Z_{even}^{j,1} \\
& + (g Z_-^{k,2+I} Z_+^{i,1} - l_I Z_-^{k,2} Z_+^{i,2+I}) Z_{even}^{j,2+I}] P_L \\
& - \frac{i}{\sqrt{2}} [g Z_-^{*i,2} Z_+^{*k,1} Z_{even}^{j,1} + g Z_-^{*i,1} Z_+^{*k,2} Z_{even}^{j,2} \\
& + l_I Z_-^{*i,2+I} Z_+^{*k,2+I} Z_{even}^{j,1} \\
& + (g Z_-^{*i,2+I} Z_+^{*k,1} - l_I Z_-^{*i,2} Z_+^{*k,2+I}) Z_{even}^{j,2+I}] P_R \\
H_{5+j}^0 - \kappa_i^+ - \bar{\kappa}_k^+ \;:\; & \frac{1}{\sqrt{2}} [-g Z_-^{k,2} Z_+^{i,1} Z_{odd}^{j,1} - g Z_-^{k,1} Z_+^{i,2} Z_{odd}^{j,2} + l_I Z_-^{k,2+I} Z_+^{i,2+I} Z_{odd}^{j,1} \\
& - (g Z_-^{k,2+I} Z_+^{i,1} + l_I Z_-^{k,2} Z_+^{i,2+I}) Z_{odd}^{j,2+I}] P_L \\
& - \frac{1}{\sqrt{2}} [g Z_-^{*i,2} Z_+^{*k,1} Z_{odd}^{j,1} + g Z_-^{*i,1} Z_+^{*k,2} Z_{odd}^{j,2} \\
& - l_I Z_-^{*i,2+I} Z_+^{*k,2+I} Z_{odd}^{j,1} \\
& + (g Z_-^{*i,2+I} Z_+^{*k,1} + l_I Z_-^{*i,2} Z_+^{*k,2+I}) Z_{odd}^{j,2+I}] P_R \\
H_i^+ - \kappa_j^0 - \bar{\kappa}_k^+ \;:\; & i[\frac{1}{\sqrt{2}} (Z_-^{k,2} Z_c^{i,1} + Z_-^{k,2+I} Z_c^{i,2+I}) (g Z_N^{j,2} + g' Z_N^{j,1}) \\
& - g Z_-^{k,1} (Z_c^{i,1} Z_N^{j,3} + Z_c^{i,2+I} Z_N^{j,4+I}) \\
& - l_I Z_c^{i,5+I} (Z_-^{k,2+I} Z_N^{j,3} - Z_-^{k,2} Z_N^{j,4+I})] P_L \\
& + i[-\frac{1}{\sqrt{2}} Z_+^{*k,2} Z_c^{i,2} (g Z_N^{*j,2} + g' Z_N^{*j,1}) - g Z_+^{*k,1} Z_c^{i,2} Z_N^{*j,4} \\
& - \sqrt{2} g' Z_+^{*k,2+I} Z_c^{i,5+I} Z_N^{*j,1} \\
& - l_I Z_+^{*k,2+I} (Z_N^{*j,3} Z_c^{i,2+I} - Z_N^{*j,4+I} Z_c^{i,1})] P_R
\end{aligned}
$$

$$
\begin{aligned}
H_i^0 - d^I - \bar{d}^J &: \frac{i}{\sqrt{2}} d^I Z_{even}^{i,1} \\
H_{5+i}^0 - d^I - \bar{d}^J &: \frac{1}{\sqrt{2}} d^I Z_{odd}^{i,1} \gamma_5 \\
H_i^0 - u^I - \bar{u}^J &: -\frac{i}{\sqrt{2}} u^I Z_{even}^{i,2} \\
H_{5+i}^0 - u^I - \bar{u}^J &: -\frac{1}{\sqrt{2}} u^I Z_{odd}^{i,2} \gamma_5
\end{aligned}
$$

References

[1] H. E. Haber and G. L. Kane, Phys. Rep. **117** (1985) 75

[2] H.P. Nilles, Phys. Rep. **110** (1984) 1

[3] J. Ellis, G. Gelmini, C. Jarlskog, G.G. Ross and J.W.F. Valle, Phys. Lett. **B150** (1985) 142; H. Dreiner and G.G. Ross, Nucl. Phys. **B365** (1991) 597.

[4] M. Czakon and J. Gluza, hep-ph/0003228.

[5] G. Moreau, E. Perez and G. Polesello, hep-ph/0003012.

[6] J. Ellis, J. Hagelin, D.V. Nanopoulos, K. Olive and M. Srednicki, Nucl. Phys. **B238** (1984) 453.

[7] Wan Lan-Hui, Ma Wen-Gan, Yin Xi, Jiang Yi and Han Liang, J. of Phys. **G27** (2001)203.

[8] M. Chaichian, K. Huitu and Z.-H. Yu, hep-ph/0101272.

[9] C.H. Chang and T.F. Feng, Eur.Phys.J. **C12** (2000)137; hep-ph/9908295.

[10] R. Barbier et al., hep-ph/9810232.

[11] V. Telnov, Nucl. Instrum. Methods Phys.Rev. **A294** (1990) 72; L. Ginzburg, G. Kotkin and H. Spiesbergerm, Fortschr. Phys. **34** (1986) 687.

[12] K. Cheung, Phys. Rev. **D47** (1993) 3750; **50** (1994)1173.

[13] Particle Data Group, R.M. Barnett et al., Phys. Rev. **D50** (1994) 1.

Figure captions

Fig.1 The $\not{R}_p$ MSSM one-loop order diagrams contributing to the $\gamma\gamma \to \tilde{\chi}_1^+\tau^-$. (a) self-energy diagrams; (b) vertex diagrams; (c) s-channel diagrams; (d) box diagrams, and (e) quartic coupling diagrams. The H^0, H^-, κ^+, κ^0 denote the corresponding particles as we have given in Eq.(12)-(19). d, u, $\tilde{D}$, $\tilde{U}$ denote quarks and squarks respectively, where only the third generation is considered for convenience. The diagrams with incoming photons exchanged are not shown in the figures.

Fig.2 The $\gamma\gamma$ subprocess cross section as functions of $\sqrt{\hat{s}}$, with $\mu = 370\ GeV$, mass of $\tilde{\chi}_1$ at 90 GeV, 110 GeV and 170 GeV, denoted by the solid line, the dashed line and the dotted line respectively.

Fig.3 Both cross sections of the $e^+e^- \to \gamma\gamma\tilde{\chi}_1^+\tau^-$ process and the $e^+e^- \to \tilde{\chi}_1^+\tau^-$ tree level process as the functions of $\sqrt{\hat{s}}$, with $\mu = 370\ GeV$. Contributions from only bilinear $\not{R}_p$ terms with mass of $\tilde{\chi}_1$ at 90 GeV, 110 GeV and 170 GeV are plotted, denoted by the solid line, the dashed line and the dotted line respectively.

Fig.4 The cross section of the e^+e^- process as unctions of the final chargino mass $m_{\tilde{\chi}1}$, which ranges from 90 GeV to 200 GeV. The solid line and the dashed line are for $\sqrt{\hat{s}} = 500\ GeV$ and $\sqrt{\hat{s}} = 1\ TeV$ respectively.

Fig.5 The cross section of the e^+e^- process as functions of μ, which is assumed positive and ranges from 100 GeV to 300 GeV. The solid line and the dashed line are for $\sqrt{\hat{s}} = 500\ GeV$ and $\sqrt{\hat{s}} = 1\ TeV$ respectively.

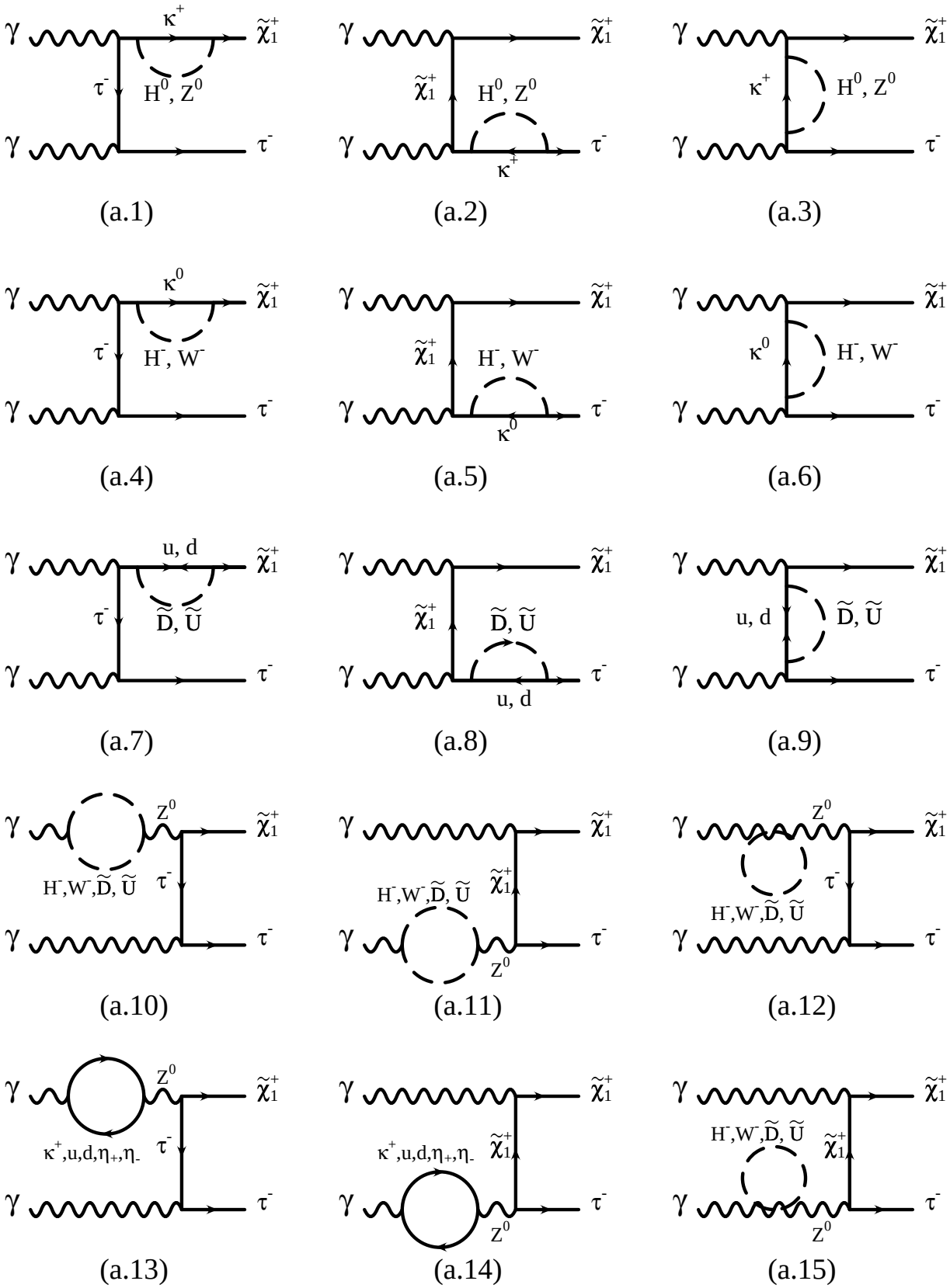
γ
γ
κ^+
$\tilde{\chi}_1^+$
τ^-
H^0, Z^0
(a.1)
$\tilde{\chi}_1^+$
H^0, Z^0
κ^+
(a.2)
κ^+
H^0, Z^0
(a.3)
κ^0
H^-, W^-
(a.4)
κ^0
(a.5)
(a.6)
u, d
$\widetilde{D}, \widetilde{U}$
(a.7)
u, d
(a.8)
(a.9)
Z^0
$H^-,W^-,\widetilde{D}, \widetilde{U}$
(a.10)
(a.11)
(a.12)
$\kappa^+,u,d,\eta_+,\eta_-$
(a.13)
(a.14)
(a.15)

Fig.1(a)

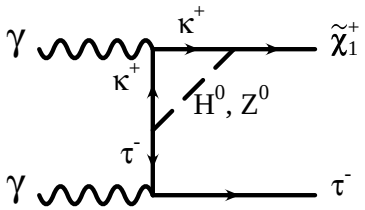

(b.1)

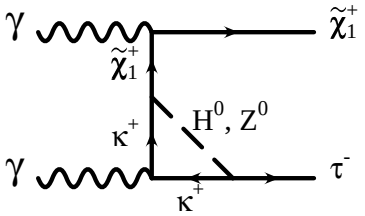

(b.2)

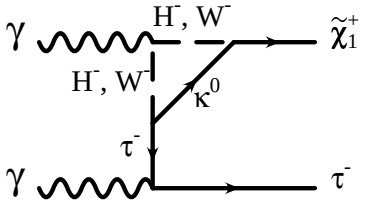

(b.3)

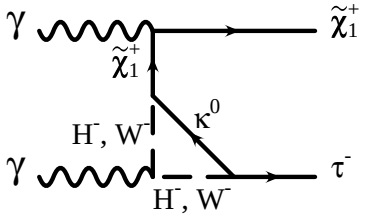

(b.4)

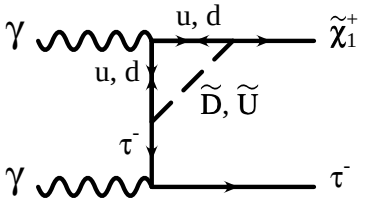

(b.5)

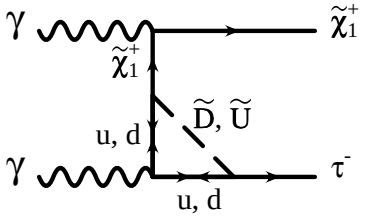

(b.6)

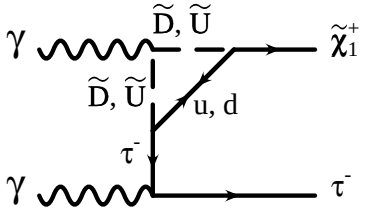

(b.7)

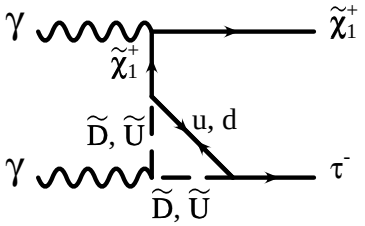

(b.8)

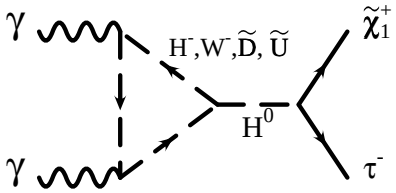

(c.1)

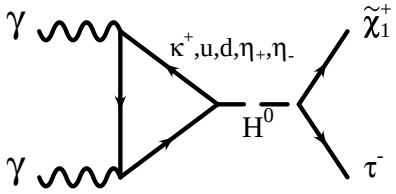

(c.2)

Fig.1(b,c)

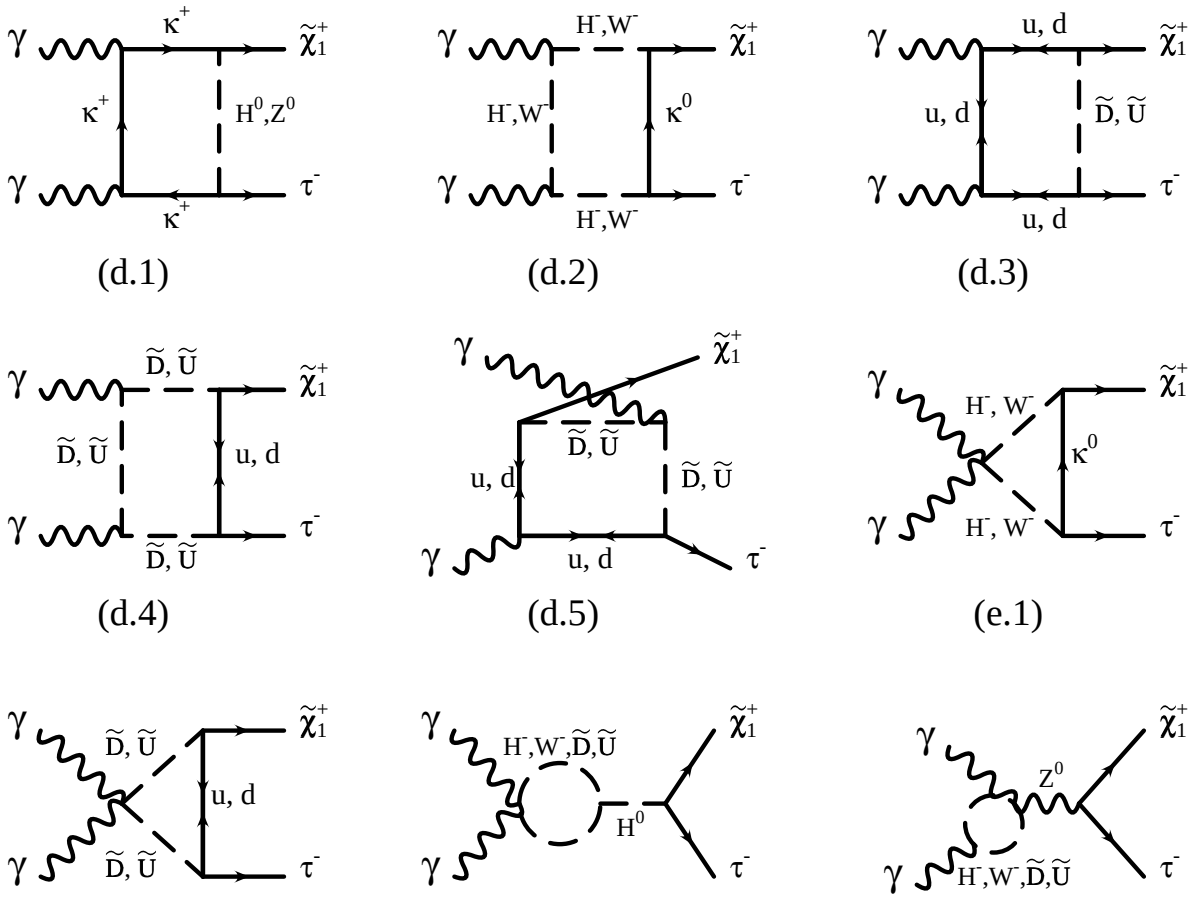
γ
κ+
$\tilde{\chi}_1^+$
κ+
H0,Z0
γ
τ-
κ+
(d.1)
H-,W-
$\tilde{\chi}_1^+$
H-,W-
κ0
γ
τ-
H-,W-
(d.2)
u, d
$\tilde{\chi}_1^+$
u, d
D̃, Ũ
γ
τ-
u, d
(d.3)
D̃, Ũ
$\tilde{\chi}_1^+$
D̃, Ũ
u, d
γ
τ-
D̃, Ũ
(d.4)
γ
$\tilde{\chi}_1^+$
D̃, Ũ
u, d
D̃, Ũ
γ
τ-
u, d
(d.5)
γ
H-, W-
$\tilde{\chi}_1^+$
κ0
γ
τ-
H-, W-
(e.1)
γ
D̃, Ũ
$\tilde{\chi}_1^+$
u, d
γ
τ-
D̃, Ũ
(e.2)
γ
H-,W-,D̃,Ũ
$\tilde{\chi}_1^+$
H0
γ
τ-
(e.3)
γ
Z0
$\tilde{\chi}_1^+$
γ
H-,W-,D̃,Ũ
τ-
(e.4)

Fig.1(d,e)

Fig.2

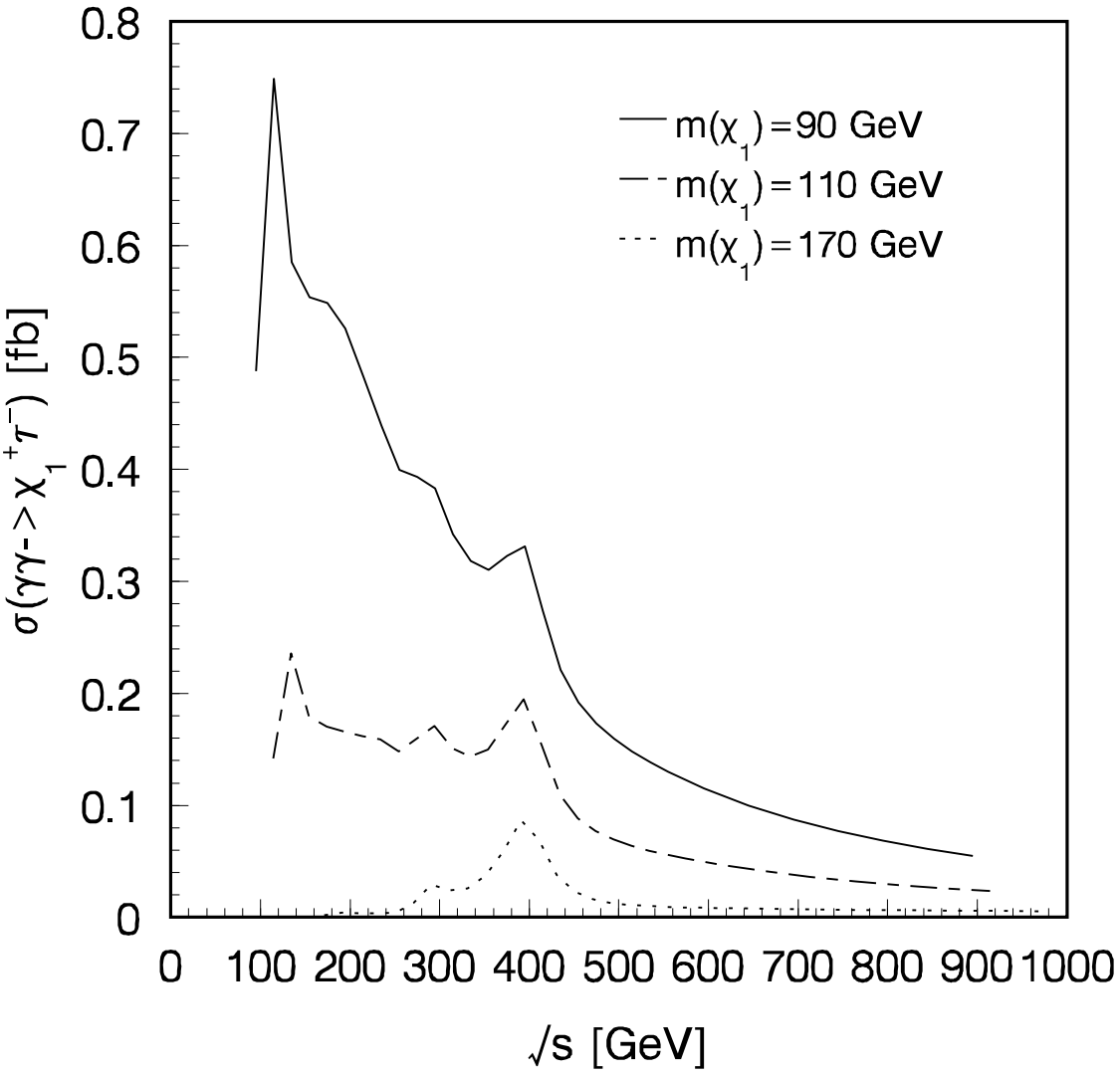
0.8
0.7
0.6
0.5
0.4
0.3
0.2
0.1
0
σ(γγ->χ1+τ−) [fb]
m(χ1)=90 GeV
m(χ1)=110 GeV
m(χ1)=170 GeV
0 100 200 300 400 500 600 700 800 900 1000
√s [GeV]

Fig.3

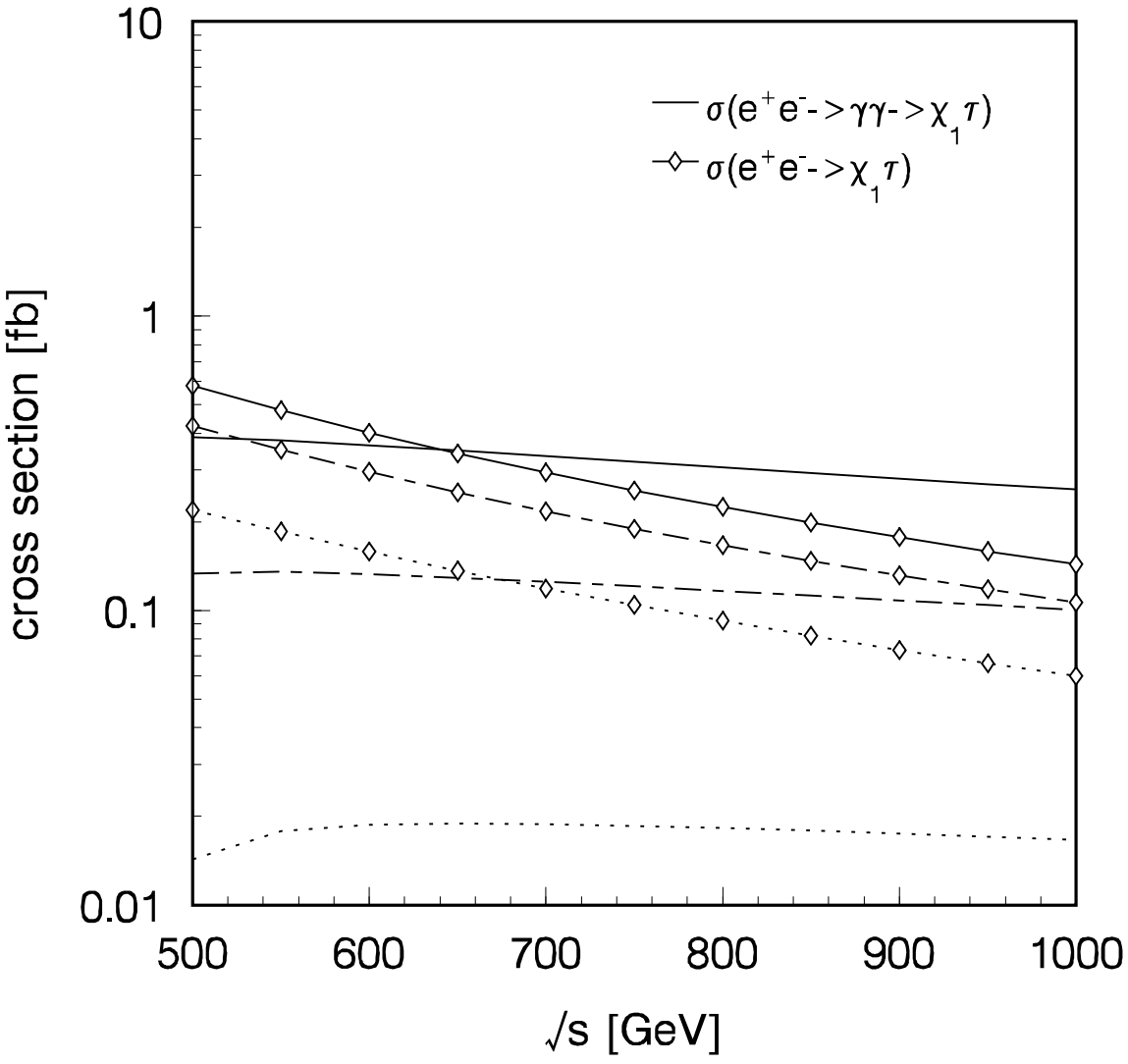
10
1
0.1
0.01
cross section [fb]
500
600
700
800
900
1000
√s [GeV]
σ(e+e- -> γγ -> χ1τ)
σ(e+e- -> χ1τ)

Fig.4

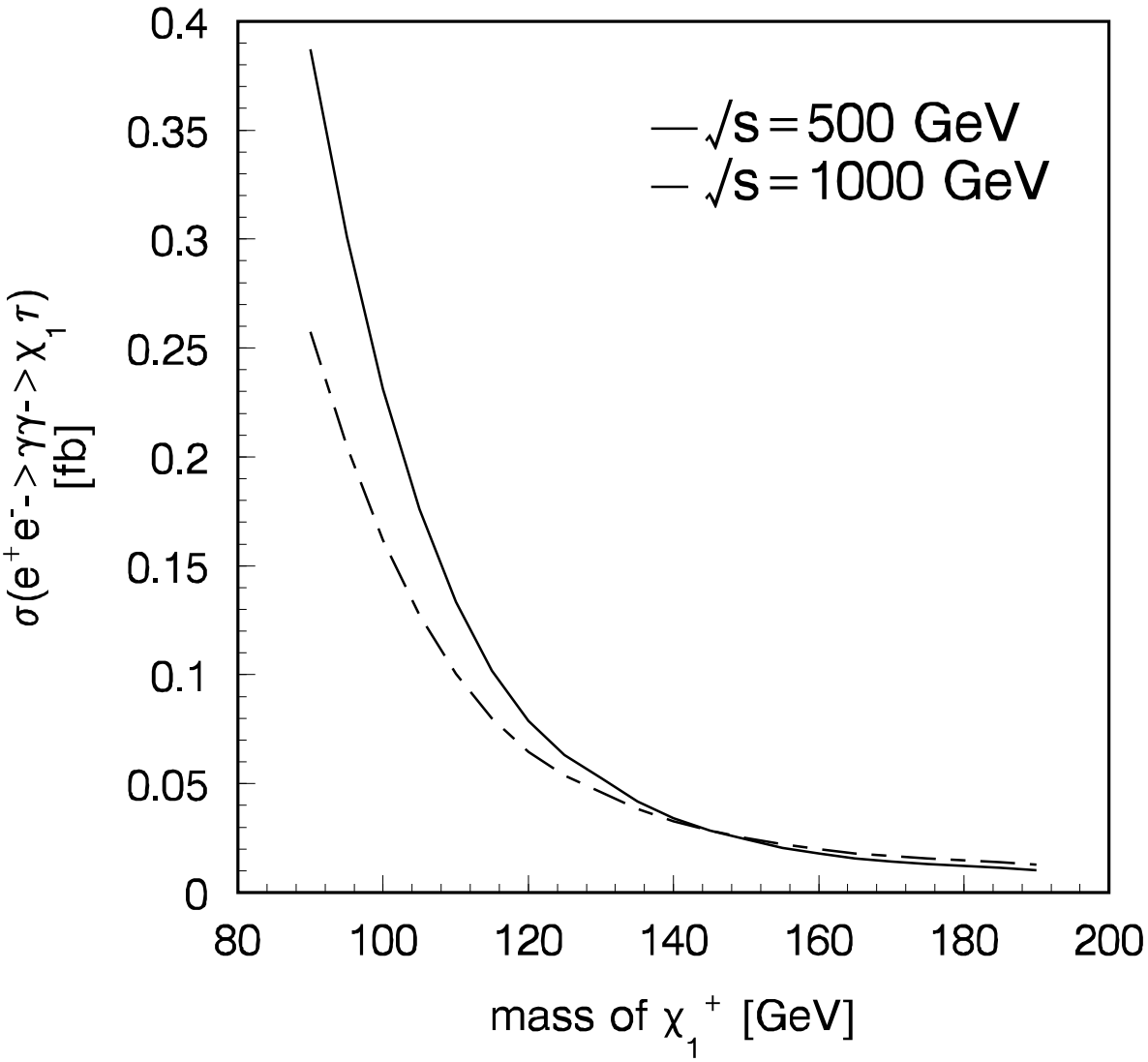
0.4
0.35
0.3
0.25
0.2
0.15
0.1
0.05
0
80
100
120
140
160
180
200
— √s = 500 GeV
— √s = 1000 GeV
σ(e+e- -> γγ- -> χ1+ τ) [fb]
mass of χ1+ [GeV]

Fig.5

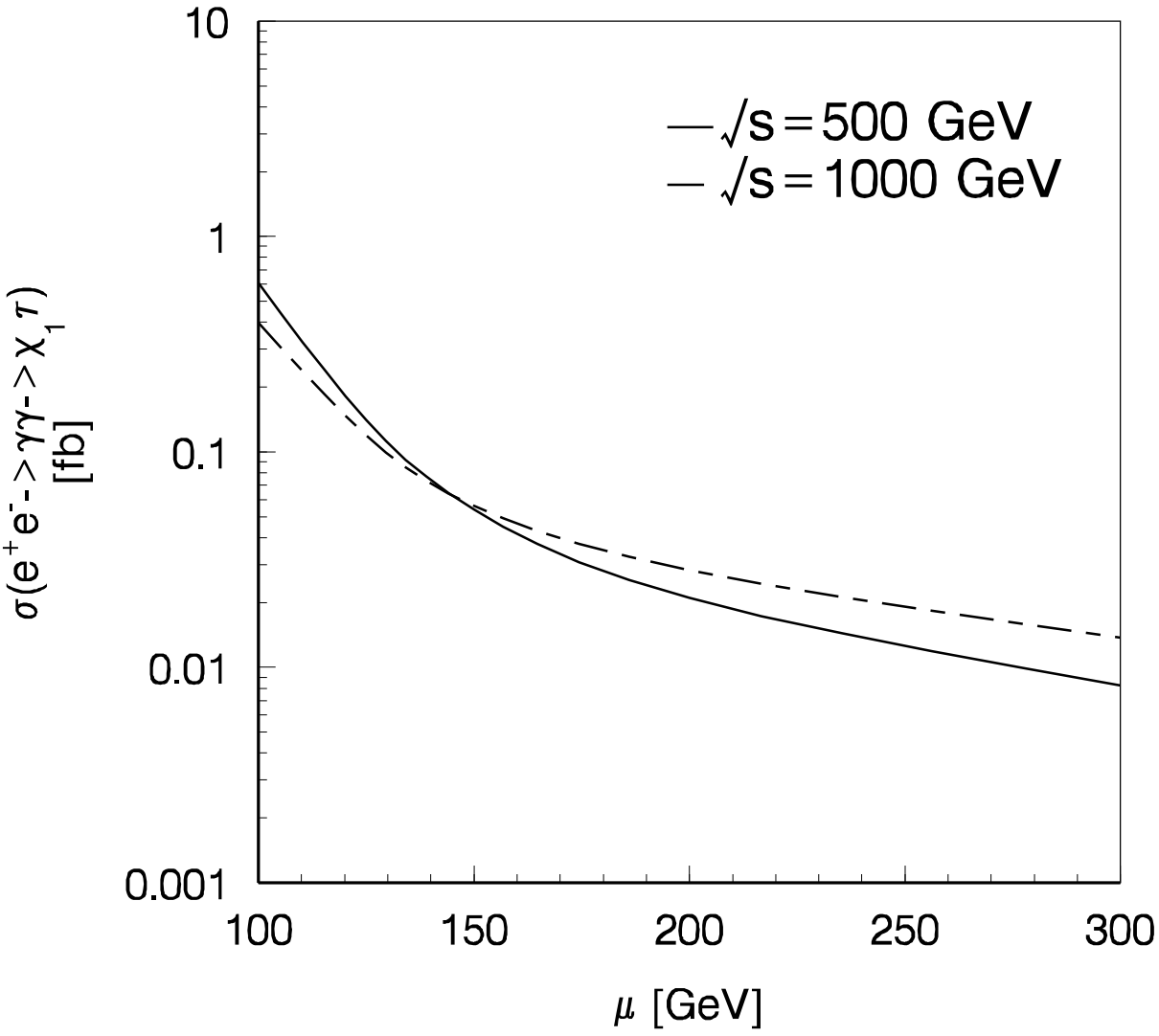
10
1
0.1
0.01
0.001
100
150
200
250
300
— √s = 500 GeV
— √s = 1000 GeV
σ(e+e- -> γγ- -> χ1 τ) [fb]
μ [GeV]